Tetrahedron 66 (2010) 4223–4229

Contents lists available at ScienceDirect

Tetrahedron

journal homepage: www.elsevier.com/locate/tet

# Donor–acceptor organic sensitizers assembled with isoxazole or its derivative 3-oxopropanenitrile

Yi-Tsung Li [a], Chao-Ling Chen [a], Yu-Yen Hsu [a], Hui-Chu Hsu [a], Yun Chi [a,*], Bo-So Chen [b], Wei-Hsin Liu [b], Cheng-Hsuan Lai [b], Tsung-Yi Lin [b], Pi-Tai Chou [b,*]

[a] Department of Chemistry, National Tsing Hua University, Hsinchu 30013, Taiwan, People's Republic of China
[b] Department of Chemistry, National Taiwan University, Taipei 106, Taiwan, People's Republic of China

ARTICLE INFO

*Article history:*
Received 28 January 2010
Received in revised form 16 March 2010
Accepted 23 March 2010
Available online 27 March 2010

*Keywords:*
Dye-sensitized solar cell
Dithiophene
Isooxazole
Cyanoacetic acid

ABSTRACT

A series of new donor–acceptor organic sensitizers **LJ5**–**LJ7** assembled with isoxazole or its derivative 3-oxopropanenitrile was synthesized and used in dye-sensitized solar cells to study the effect of both π-spacers and anchoring groups on device performance. X-ray crystal structure analyses show planar arrangement of dithiophene and isoxazole fragments, providing an excellent π conjugation and hence the large electronic coupling between the triphenylamine donor and electron acceptor units. For the DSSC applications, the derived photophysical and photovoltaic properties revealed a lower $\eta$ value of 1.06% (**LJ7**) and 2.41% (**LJ5**), and 3.30% (**LJ7**) for the dyes with rhodanine-3-acetic acid, cyanoacetyl group, and vinyl cyanoacetic acid as the anchor. Electrochemical impedance spectroscopy was used to determine the interfacial charge transfer process occurring in solar cells that employed different dyes.


## 1. Introduction

The dye-sensitized solar cells (DSSCs) have attracted considerable attention as a promising photovoltaic technology during the past two decades owing to their prospect of high energy conversion efficiency and low production costs.[1] Upon optimization, a few photosensitizers based on ruthenium metal complexes have nowadays achieved solar-to-electric power conversion efficiency $\eta$, over 10–11% under AM 1.5 irradiation.[2] Due to the relatively high cost of ruthenium element, numerous research groups have expended endeavors to develop metal free organic dyes as the alternative sensitizers.[3] As a result, impressive photovoltaic performances have been reported on various tailor-made organic dyes, which include coumarin,[4] indoline,[5] oligoene,[6] merocyanine,[7] hemicyanine,[8] perylene,[9] and xanthene,[10] showing promising $\eta$ values in the range of 5–9.8%.

Majority of the aforementioned organic sensitizers could be considered as electron donor–π-conjugated-acceptor (D–π-A) compounds.[11] Due to the π-orbital overlapping, the coupling matrix between neutral and charge transfer (zwitterion) species is normally>>kT. Thus, upon electronic excitation, fast, barrierless type of intramolecular charge transfer takes place, which is commonly named as adiabatic type of optical electron transfer.[12] Upon ingenious design of D/A chromophores as well as the π-spacer that may also serve as an antenna, the lower lying electron transfer absorption bands could be broad, intense in the visible region, which is pivotal for producing a large photocurrent response. The resulting electron (or charge) transfer to the acceptor group may subsequently facilitate rapid electron injection from the sensitizers into the conduction band of a wide band-gap semiconductor, such as $TiO_2$, the process of which is essential for making efficient DSSCs. Among various compositions that constitute these D–π-A organic sensitizers, it has been demonstrated that triphenylamine (TPA),[13] thiophene based aromatics,[14] and cyanoacetic acid[15] (or even rhodanine-3-acetic acid)[16] are the effective electron donating moiety, π-conjugated spacer and electron acceptor (anchoring group), respectively. Notable bathochromatic shift and increase of the molar extinction coefficient of the absorption spectra could be further achieved by functionalization of these units such as to develop an extended π-framework, showing direct influence of the molecular architecture on the DSSCs performances.

In this study, we initiated a project via seminally exploiting the electron-deficient isoxazole fragment as part of the π-spacer suited for DSSCs. Despite the fact that isoxazole is well-known for its great electron transporting property in OLED applications,[17] it has never been tested and utilized for preparation of DSSC sensitizers. One of our aims is to gain a better understanding of the relationship between molecular structures and elemental properties of organic sensitizers in DSSC applications. Herein, we report on the synthesis and characterization of both cyanoacetic acid and rhodanine-3-acetic acid derivatives with unprecedented bithiophene–isoxazole

* Corresponding authors. E-mail address: ychi@mx.nthu.edu.tw (Y. Chi).

0040-4020/$ – see front matter 
doi:10.1016/j.tet.2010.03.085

spacer (compounds **1**–**4**). Single crystal X-ray diffraction study on one intermediate compound **3** was also conducted to reveal the skeletal arrangement of the bithiophene–isoxazole unit. This π-conjugated-acceptor part is then linked with TPA as the electron donor unit,[13,18] due to its wider applicability to establish an integrated donor–π-acceptor framework, i.e., compounds **LJ6** and **LJ7**, suited for DSSCs. Amid the study, we also accidentally generated a 3-oxopropanenitrile anchoring group (**LJ5**) during a futile attempt to synthesize the carboxyl substituted isoxazole fragment upon employing base catalyzed ester hydrolysis. DSSCs with fair to good performance characteristics were successfully fabricated using these organic sensitizers.

## 2. Results and discussion

The organic dyes **LJ5**, **LJ6**, and **LJ7** were prepared by a synthetic protocol illustrated in Scheme 1. The targeted dyes are synthesized in multi-step procedures from a bithiophene derivative, namely 1-(5′-bromo-2,2′-bithiophen-5-yl) ethanone. Compound **1** was synthesized employing Claisen condensation with diethyl oxalate to form β-diketone, followed by the hydroxylamine cyclization. Compound **2** was next obtained by treatment of **1** with lithium tri-*tert*-butoxyaluminohydride to afford a hydroxymethyl intermediate, followed by selective oxidation employing pyridinium chlorochromate to form the anticipated carbaldehyde. After then, both compounds **1** and **2** were treated with 4-(diphenylamino) phenylboronic acid in the presence of $Pd(PPh_3)_4$ to afford TPA substituted derivatives **3** and **4**, respectively. Organic dye **LJ5** was then synthesized from **3** upon treatment of NaOH in methanol, while **LJ6** and **LJ7** were successfully synthesized via condensation of **4** with cyanoacetic acid under Knoevenagel condition and with rhodanine-3-acetic acid, respectively.

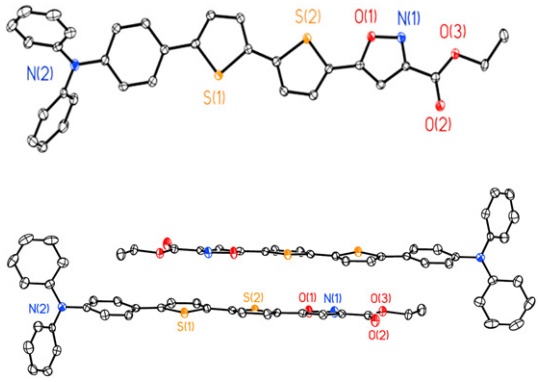


**Figure 1.** Crystallographic structure of compound **3**.

Identification of the organic dyes **LJ5**–**LJ7** were next achieved according to their spectroscopic data and microanalysis. Particularly noteworthy is the generation of **LJ5** dye via the NaOH catalyzed decarboxylative ring opening and cleavage of isoxazole

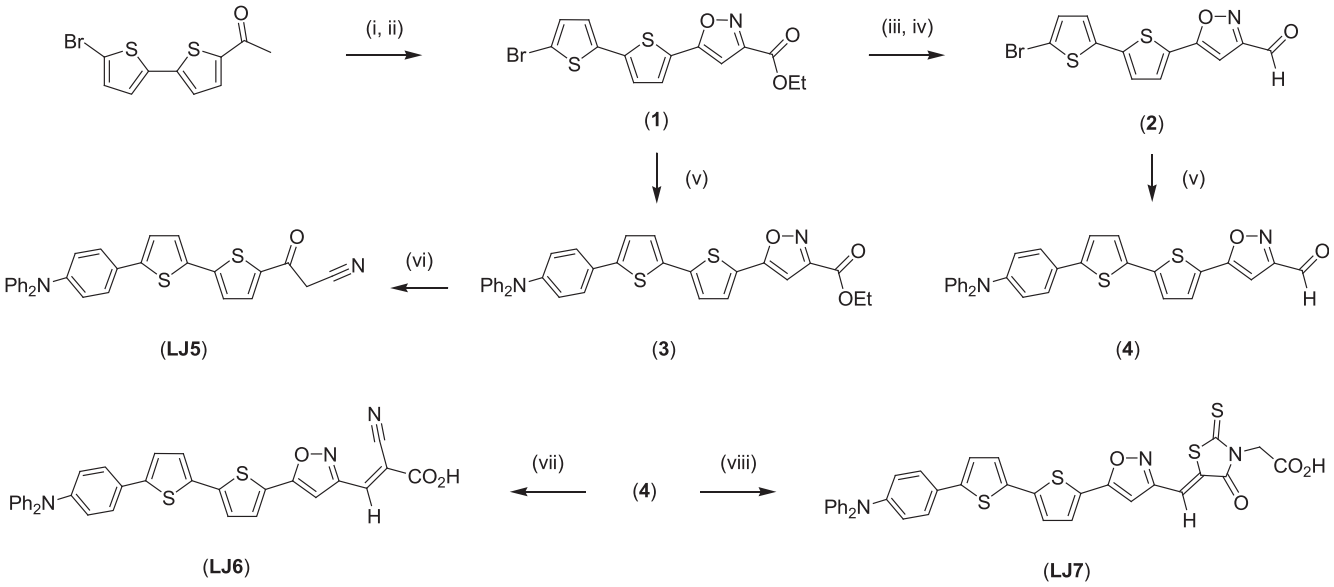


**Scheme 1.** Synthetic route to the sensitizers **LJ5**, **LJ6**, and **LJ7**; conditions: (i) $(CO_2Et)_2$, NaOEt, (ii) $H_2NOH{\cdot}HCl$, (iii) $LiAl(O^tBu)_3H$, (iv) PCC, RT, (v) DPBA, $Pd(PPh_3)_4$, $K_2CO_3$, reflux, (vi) NaOH, MeOH, 12 h, (vii) CAA, $NH_4OAc$, HOAc, (viii) RAA, $NH_4OAc$, HOAc.

Single crystal X-ray diffraction study on compound **3** was examined in an aim to unravel the relative geometry between dithiophene and isoxazole fragments. As shown in Figure 1, the side view clearly shows the minimal deviation of torsional angles from planarity (≤2°). In theory, such planar configuration is expected to provide excellent π conjugation and hence the large electron coupling between the donor and the acceptor units. Conversely, terminal phenyl substituents of the triphenylamine group are arranged in a nearly perpendicular fashion, the result of which renders maximum steric hindrance to block the approaching of other molecules. In fact, careful examination of the crystal-packing diagram of **3** indicates the adaptation of a head-to-tail placement with an average separation of 3.8 Å between the π spacer of adjacent molecules. This nearly non-bonding distance could explain the absence of ππ stacking interaction in its crystal lattices, and serve as a model to eliminate similar interaction on the $TiO_2$ surface after the impregnation and deposition of relevant dyes.

fragment of **3**.[19] Note that **LJ5** possesses a unique cyanoacetyl group, which is also suited for anchoring on $TiO_2$ (vide infra). Identification of the **LJ5** dye was provided by the observation of a methylene singlet at $\delta$ 3.93 in the $^1H$ NMR spectrum as well as the detection of $\nu$(C≡N) stretching band at 2254 $cm^{-1}$ in its IR spectrum.

The UV–vis absorption and emission spectra of **LJ5**–**LJ7** dyes in *N*,*N*-dimethyformamide (DMF) are shown in Figure 2, and the

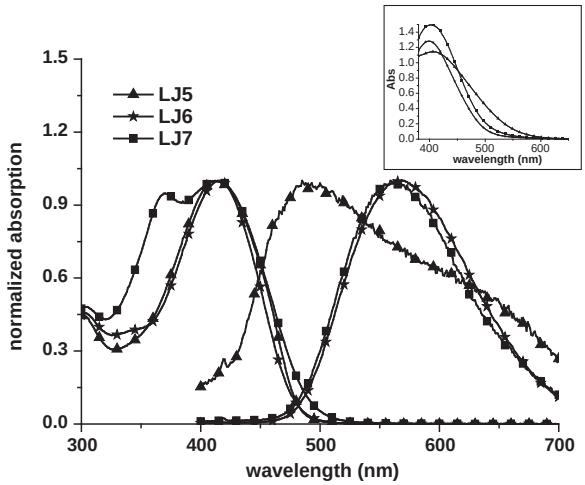


**Figure 2.** The UV/Vis and emission spectra of **LJ5**, **LJ6**, and **LJ7** dyes in DMF solution. Sample is excited at the lowest energy absorption maximum. Insert: The film UV–vis absorption on 6 μm thickness $TiO_2$ thin film.

corresponding data were collected in Table 1, particularly the absorption peak wavelengths on the $TiO_2$ surface, which are essential for identifying the respective bonding interaction. In general, **LJ5**–**LJ7** showed the maximum absorption wavelength ($\lambda_{abs}$) at 412, 416, and 414 nm, respectively, which were corresponding to HOMO (highest occupied molecular orbital)/LUMO (lowest unoccupied molecular orbital) type of $\pi\pi^*$ transition. When **LJ5**–**LJ7** were anchored on the $TiO_2$ surface, the absorption maxima of these dyes were only blue-shifted by 5, 17, and 12 nm in comparison to those in solution, respectively, a result generally attributed to the deprotonation of the carboxylic acid.[20] However, the onset of the lowest lying absorption for three dyes all tails down to ~600 nm. This is plausibly due to the electronic interaction with electron deficient $TiO_2$, lowering the corresponding energy gap.[21,6b] In DMF, both **LJ6** and **LJ7** exhibited distinct emission band with peak wavelength centered at 570 and 559 nm, respectively. The large stokes shift of $>8000\ cm^{-1}$ in DMF between absorption and emission maxima manifests the strong charge transfer character, being expected via their original design strategy. Dual emission was resolved for **LJ5**, consisting of a band maximized at ~490 nm and a distinct shoulder at ~600 nm. Upon monitoring at emission wavelength at, e.g., 500 nm, an excitation peak wavelength of 400 nm was resolved, while a peak wavelength of ~440 nm was observed upon monitoring at, e.g., 650 nm (see Fig. S1 in Supplementary data). Since **LJ5** has an acidic methylene unit, that is, linked by the electron withdrawing carbonyl and cyano groups, the occurrence of keto-enol tautomerization is plausible (see Scheme 2). The enol-form, due to its longer π-conjugation, should possess lower energy gap as well as stronger charge transfer properties, resulting in the ~600 nm emission in DMF. This viewpoint is supported by the observation of keto-form only emission maximized at ~500 nm in cyclohexane (see Fig. S2 of Supplementary data).

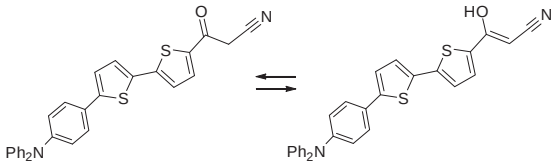


**Scheme 2.** Proposed keto-enol tautomerization involving the sensitizer **LJ5**.

To further study the possibilities of electron injection from the excited state dye to conduction band (CB) of semiconductor and the dye regeneration, the CV of these dyes was performed in acetonitrile to measure the redox potentials. The first oxidation potentials ($E_{ox}$) corresponding to the HOMO levels of the dyes were summarized in Table 1. The HOMO levels of **LJ5**, **LJ6**, and **LJ7** dyes are calculated to be 0.75, 0.82, and 0.79 V, respectively, which are positive enough comparing with that of iodine/iodide (0.4 V),[22] indicating that the oxidized dyes could be reduced effectively by electrolyte and then regenerated. Moreover, the HOMO level is mainly affected by electron donor. Thus, from the HOMO level data of these dyes, it is not too surprising for the observation of only a minor change in HOMO level among these dyes.

On the other hand, the LUMO levels can be estimated from their respective HOMO level and the $S_0 \rightarrow S_1$ (0,0) vibronic onset energy of the dyes; the latter is calculated from the intersection between the absorption and emission spectra ($E_{0-0}$) obtained in solution. These obtained HOMO and LUMO energy levels of dyes are also summarized in Table 1. It is notable that, for effectively injecting the electron into the conduction band of $TiO_2$, the LUMO levels of the dyes must be sufficiently more negative than the conducing band energy ($E_{cb}$) of $TiO_2$ semiconductor, (−0.5 V vs NHE).[22] The corresponding values of these organic dyes are calculated to be −1.98, −1.76, and −1.76 V for **LJ5**, **LJ6**, and **LJ7**, respectively. Furthermore, the larger energy gaps between the LUMO of the organic sensitizers and $E_{cb}$ of semiconductor are not only sufficient for efficient electron injection, but also allowing the employment of 4-*tert*-butylpyridine (TBP) as the additive, which shift the $E_{cb}$ of the $TiO_2$ negatively and improve the open-circuit voltage and total conversion efficiency consequently.[23]

The photovoltaic properties of the solar cells fabricated with these organic dyes were measured under simulated AM 1.5 G irradiation ($100\ mW\ cm^{-2}$). A 12+4 μm thickness of $TiO_2$ film was used for fabrication of DSSCs, where the first and second digits indicate the thickness of dye adsorption and light scattering layers, respectively. The sensitization was conducted employing a $3\times10^{-4}$ M of dye solution in DMF and 1 mM of deoxycholic acid (DCA) for a period of 10 h. The electrolyte contains 0.6 M 1-butyl-3-methylimidazolium iodide (BMII), 0.1 M LiI, 0.05 M $I_2$, 0.5 M 4-*tert*-butylpyridine (TBP), 0.1 M guanidinium thiocyanate in dry acetonitrile. The open-circuit voltage ($V_{OC}$), short-circuit current density ($J_{SC}$), fill factor (FF), and solar energy-to-electricity conversion efficiencies ($\eta$) were listed in Table 2. Photocurrent density–voltage ($J$–$V$) characteristics of these dyes are depicted in Figure 3.

Depending on the dyes selected, our DSSCs showed moderate performance data. The DSSC based on **LJ7** dye gave a lower $\eta$ value

**Table 1**
Photophysical and electrochemical data of **LJ5**, **LJ6**, and **LJ7** dyes

| Dye | $\lambda_{abs}$, nm (ε, $M^{-1}\ cm^{-1}$)[a] | $\lambda_{abs}$ on $TiO_2$, nm | $\lambda_{em}$,[a] nm | Potentials and energy levels | | |
|---|---|---|---|---|---|---|
| | | | | $E_{ox}$,[b] V | $E_{0-0}$,[c] V | $E_{ox}-E_{0-0}$, V |
| **LJ5** | 412 (41,553) | 407 | 485 | 0.75 | 2.73 | −1.98 |
| **LJ6** | 416 (38,820) | 399 | 570 | 0.82 | 2.58 | −1.76 |
| **LJ7** | 414 (45,673) | 402 | 559 | 0.79 | 2.55 | −1.76 |

[a] Absorption and emission spectra were measured in DMF solution.
[b] The oxidation potentials of dyes on $TiO_2$ were measured in $CH_3CN$ with 0.1 M tetrabutylammonium hexafluorophosphate (TBAP) with a scan rate of $50\ mV\ s^{-1}$ versus normal hydrogen electrode (NHE).
[c] $E_{0-0}$ was determined from the intersection of absorption and emission spectra.

**Table 2**
The photovoltaic data of DSSCs based on **LJ5**, **LJ6**, and **LJ7** dyes

| Dye | $J_{SC}$ (mA cm$^{-2}$) | $V_{OC}$ (mV) | *FF* | $\eta$ (%) |
|---|---|---|---|---|
| **LJ5** | 7.74 | 491 | 63.5 | 2.41 |
| **LJ6** | 8.04 | 662 | 62.0 | 3.30 |
| **LJ7** | 3.60 | 457 | 64.4 | 1.06 |

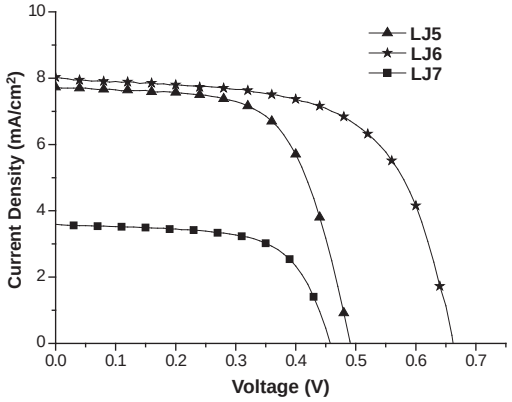


**Figure 3.** The J–V curves of DSSCs based on **LJ5**, **LJ6**, and **LJ7** dyes.

of 1.06%, together with $J_{SC}$=3.60 mA cm$^{-2}$, $V_{OC}$=457 mV, *FF*=0.644. The lower IPCEs obtained for **LJ7** could be attributed to the result of the LUMO being located in a rhodanine framework rather than at the carboxylic acid group. As a result, a decrease of the electron injection efficiency in a dynamic manner is expected.[24] Next, the DSSC based on **LJ5** dye exhibited an improved $\eta$ value of 2.41%, together with $J_{SC}$=7.74 mA cm$^{-2}$, $V_{OC}$=491 mV, *FF*=0.635, despite of the fact that the **LJ5** dye contained no carboxylic acid linker. On this basis, the adsorption of **LJ5** onto $TiO_2$ is more plausibly via its enol group, together with the cyano group, indirectly supporting the existence of enol-form for **LJ5** in DMF (vide supra). It is obvious that the nearly twofold improvement in $\eta$ value of **LJ5** cell versus that of **LJ7** is due to the stronger association of enolic OH group to the $TiO_2$ semiconductor surface. Thus the electron injection could occur from the excited state dye to the conduction band of $TiO_2$ nanoparticles via the enolic OH group. Such an observation has been recently reported for the kaede dye with hydroxy group as the anchoring group.[25] Finally, the best DSSC is fabricated employing **LJ6**, for which the device performance data are $\eta$=3.30%, $J_{SC}$=8.07 mA cm$^{-2}$, $V_{OC}$=662 mV, *FF*=0.63, showing the best anchoring capability among all three sensitizers, attributed to the cyanoacetic acid group.

The incident photon-to-current conversion efficiencies (IPCEs) of these DSSC dyes are shown in Figure 4. The onset of the IPCE spectra of **LJ5** and **LJ6** is ~600 nm, and high IPCE performance (>60%) was observed from the region of 440–480 nm. In contrast, the IPCE spectra of DSSC in **LJ7** exhibited much lower IPCE maxima of 39% at ~445 nm. The rather low IPCE values for this dye reflect lower photocurrent and hence inferior photovoltaic performance. The results may further imply that rhodanine-3-acetic acid is a poor anchor in comparison to cyanoacetic acid, at least, in these oxazole analogs.

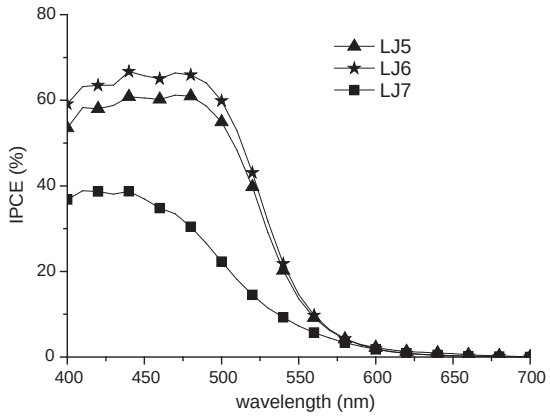


**Figure 4.** IPCE spectra of DSSCs based on **LJ5**, **LJ6**, and **LJ7** dyes.

To verify this viewpoint, we then fabricated devices using **LJ6** and **LJ7** dye for electrochemical impedance measurements. According to the Bode phase plot (see Fig. 5 below) performed with potentiostat/glavanostat (PGSTAT 12, AUTOLAB), the Bode phase plot of two representative devices **LJ6** and **LJ7** indicates that the characteristic frequency of device LJ6 (~22 Hz) is lower than that of device **LJ7** (~126 Hz). The results provide supplementary support in that the electron lifetime is shorter in device **LJ7**.[26] This can be ascribed to certain degrees of the disruption of the $\pi$* electron conjugation between rhodanine and the carboxylic acid (due to the addition of a methylene group in between) in **LJ7**, resulting in a decrease of the electron injection efficiency.

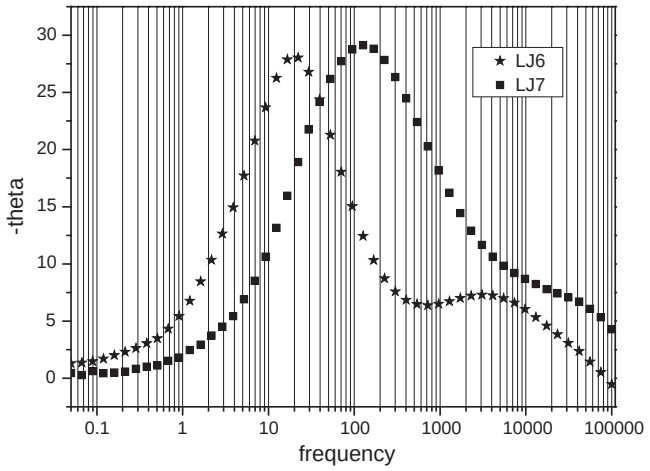


**Figure 5.** Bode phase plot of device **LJ6** and **LJ7** at open-circuit condition under **1** sun solar irradiation.

## 3. Conclusions

To sum up, we have demonstrated the exploitation of the electron-deficient isoxazole fragment as portion of the $\pi$-spacer and the electron acceptor suited for DSSCs. Moderate conversion efficiency has been achieved. The inferiority of cell performance at current stage is due to the limit in the harvesting mainly on $\leq$550 nm of solar photons. This obstacle should be circumvented via the feasibility and versatility in its future derivatization.

## 4. Experimental

### 4.1. General methods

All reactions were performed under nitrogen atmosphere and solvents were distilled from appropriate drying agents prior to use. Commercially available reagents were used without further purification unless otherwise stated. All reactions were monitored using pre-coated TLC plates (0.20 mm with fluorescent indicator UV254). Mass spectra were obtained on a JEOL SX-102A instrument operating in electron impact (EI) or fast atom bombardment (FAB) mode. $^{1}$H and $^{13}$C NMR spectra were recorded on a Varian Mercury-400 or an INOVA-500 instrument. Elemental analysis was carried

out with a Heraeus CHN–O Rapid Elementary Analyzer. 1-(5′-Bromo-2,2′-bithiophen-5-yl) ethanone was prepared from *N*-bromosuccinimide (NBS) and (2,2′-bithiophen-5-yl) ethanone according to the literature procedure.[27]

*4.1.1. Ethyl 5-(5′-bromo-2,2′-bithiophen-5-yl) isoxazole-3-carboxylate (**1**).* A mixture of 1-(5′-bromo-2,2′-bithiophen-5-yl) ethanone (500 mg, 1.74 mmol) and diethyl oxalate (500 mg, 3.48 mmol) was stirred in 5 mL of THF at rt for ten minutes, followed by addition of sodium ethoxide (NaOEt, 240 mg, 3.52 mmol). After stirring for 12 h, the solution was quenched by addition of 2 N HCl solution to a pH value of 3–4. The yellow precipitate was collected, rinsed with water, and dried under vacuum. This material was then mixed with hydroxylamine hydrochloride (540 mg, 7.8 mmol) in EtOH (30 mL) and the solution was refluxed for 12 h. After cooling to rt, solvent was then removed and the residue was purified by silica gel column chromatography eluted with a 4:1 mixture of hexane and $CH_2Cl_2$; yield: 414 mg, 1.08 mmol, 62%. Selected spectral data of **1**: $^1$H NMR (400 MHz, $CDCl_3$, 298 K): $\delta$ 7.43 (1H, d, $J_{HH}$=4.0 Hz), 7.10 (1H, d, $J_{HH}$=4.0 Hz), 7.00 (2H, d, $J_{HH}$=3.6 Hz), 6.75 (1H, s), 4.45 (2H, q, $J_{HH}$=7.2 Hz), 1.42 (3H, t, $J_{HH}$=7.2 Hz). $^{13}$C NMR (100 MHz, $CDCl_3$, 298 K): $\delta$ 165.9, 159.7, 156.9, 139.8, 137.3, 130.9, 128.4, 126.7, 125.0, 124.6, 112.7, 99.6, 62.3, 14.1. Anal. Calcd for $C_{14}H_{10}BrNO_3S_2$: C, 43.76; H, 2.62; N, 3.65. Found: C, 43.57; H, 2.98; N, 3.85.

*4.1.2. 5-(5′-Bromo-2,2′-bithiophene-5-yl) isoxazole-3-carbaldehyde (**2**).* THF solution of lithium tri-*tert*-butoxyaluminohydride (1.0 mL, 1.0 M) was added dropwisely to a THF (30 mL) solution of **1** (200 mg, 0.52 mmol) at rt. The mixture was heated at 50 °C for 8 h. After cooling to rt, solvent was evaporated in vacuo. The residue was dissolved into $CH_2Cl_2$, washed with water, dried over anhydrous $Na_2SO_4$, and filtered. Concentration of filtrate gave a white solid, which was then treated with pyridinium chlorochromate (PCC, 168 mg, 0.78 mmol) and $CH_2Cl_2$ (20 mL). After stirring at rt overnight, the mixture was filtered, the remaining solvent evaporated in vacuo; and the residue was purified by flash column chromatography eluting with pure $CH_2Cl_2$; yield: 159 mg, 0.47 mmol, 90%. Selected spectral data of **2**: $^1$H NMR (400 MHz, $CDCl_3$, 298 K): $\delta$ 10.14 (1H, s), 7.45 (1H, d, $J_{HH}$=3.6 Hz), 7.11 (1H, d, $J_{HH}$=3.6 Hz), 7.00 (2H, d, $J_{HH}$=3.6 Hz), 6.71 (1H, s). $^{13}$C NMR (100 MHz, $CDCl_3$, 298 K): 184.3, 166.3, 162.5, 140.1, 137.3, 130.9, 128.7, 126.5, 125.1, 124.7, 112.8, 96.0. Anal. Calcd for $C_{12}H_6BrNO_3S_2$: C, 40.46; H, 1.70; N, 3.93. Found: C, 40.27; H, 1.88; N, 3.68.

*4.1.3. Ethyl 5-(5′-(4-(diphenylamino)phenyl)-2,2′-bithiophen-5-yl) isoxazole-3-carboxylate (**3**).* 4-(Diphenylamino) phenylboronic acid (DPBA, 320 mg, 1.11 mmol) was treated with **1** (300 mg, 0.92 mmol) in presence of $Pd(PPh_3)_4$ (30 mg, 5 mol %), $K_2CO_3$ (2 N, 1.5 mL), and THF (30 mL). After refluxing for 12 h, the solvent was removed in vacuo and the residue dissolved into minimal amount of $CH_2Cl_2$. The solution was then filtered, the solvent removed, and the residue was purified by silica gel column chromatography eluting with a 4:1 mixture of hexane and $CH_2Cl_2$; yield: 499 mg, 0.72 mmol, 79%. Selected spectral data of **3**: $^1$H NMR (400 MHz, $CDCl_3$, 298 K): $\delta$ 7.44 (1H, d, $J_{HH}$=3.6 Hz), 7.43 (2H, d, $J_{HH}$=9.0 Hz), 7.27 (4H, t, $J_{HH}$=7.8 Hz), 7.19 (1H, d, $J_{HH}$=4.0 Hz), 7.16 (1H, d, $J_{HH}$=3.6 Hz), 7.14 (1H, d, $J_{HH}$=4.0 Hz), 7.11–7.03 (8H, m), 6.74 (1H, s), 4.45 (2H, q, $J_{HH}$=7.2 Hz), 1.42 (3H, t, $J_{HH}$=7.2 Hz). MS (EI): *m*/*z* 548 ($M^+$). Selected crystal data of **3**: $C_{32}H_{24}N_2O_3S_2$, *M*=548.65, monoclinic, space group *C*2/*c*, *T*=150(2) K, *a*=16.3161(12), *b*=8.7464(6), *c*=38.003(3) Å, $\beta$=93.169(2)°, *V*=5415.0(7) Å$^3$, *Z*=8, $\rho_{calcd}$=1.346 Mg/m$^3$, *F*(000)=2288, $\lambda$(Mo$K_\alpha$)=0.7107 Å, $\mu$=0.234 mm$^{-1}$, crystal size=0.30×0.25×0.05 mm$^3$, 4759 independent reflections collected ($R_{int}$=0.0658), GOF=1.192, final $R_1[I>2\sigma(I)]$=0.0736, $\omega R_2$(all data)=0.1733, and D-map, max./min.=0.519/−0.410 e/Å$^3$. Crystallographic data of **3** (excluding structure factors) was deposited in the Cambridge Crystallographic Data Centre with the deposition numbers CCDC 769595. It can be obtained free of charge on application to CCDC, 12 Union Road, Cambridge CB21EZ, UK (fax: +44 1223 336 033; e-mail: deposit@ccdc.cam.ac.uk).

*4.1.4. 5-(5′-(4-(Diphenylamino)phenyl)-2,2′-bithiophen-5-yl)isoxazole-3-carbaldehyde (**4**).* 4-(Diphenylamino) phenylboronic acid (DPBA, 102 mg, 0.35 mmol) was treated with carbaldehyde **2** (100 mg, 0.29 mmol) in presence of $Pd(PPh_3)_4$ (16 mg, 5 mol %), $K_2CO_3$ (2 N, 1.0 mL), and THF (3 mL). After the completion of the reaction, the solvent was removed in vacuo and the residue dissolved into minimal amount of $CH_2Cl_2$. It was then filtered, the solvent removed, and the residue was purified by silica gel column chromatography eluting with $CH_2Cl_2$; yield: 89 mg, 0.18 mmol, 61%. Selected spectral data of **4**: $^1$H NMR (500 MHz, $CDCl_3$, 298 K): $\delta$ 10.14 (1H, s), 7.46 (1H, d, $J_{HH}$=4.0 Hz), 7.43 (2H, d, $J_{HH}$=9.0 Hz), 7.26 (4H, t, $J_{HH}$=7.8 Hz), 7.20 (1H, d, $J_{HH}$=3.6 Hz), 7.17 (1H, d, $J_{HH}$=4.0 Hz), 7.14 (1H, d, $J_{HH}$=3.6 Hz), 7.11 (2H, d, $J_{HH}$=9.0 Hz), 7.11–7.03 (4H, m), 6.70 (1H, s). $^{13}$C NMR (125 MHz, $CDCl_3$, 298 K): $\delta$ 184.5, 166.6, 162.5, 147.8, 147.3, 144.9, 141.6, 133.9, 129.3, 128.8, 127.3, 126.5, 126.0, 125.5, 124.7, 123.9, 123.3, 123.2, 123.0, 95.6. Anal. Calcd for $C_{30}H_{20}N_2O_2S_2$: C, 71.40; H, 3.99; N, 5.55. Found: C, 71.28; H, 4.19; N, 5.33.

*4.1.5. 3-(5′-(4-(Diphenylamino)phenyl)-2,2′-bithiophen-5-yl)-3-oxopropanenitrile (**LJ5**).* Compound **3** (200 mg, 0.36 mmol) was mixed with NaOH (1 N, 1.0 mL) in MeOH (25 mL) and then refluxed overnight. After removal of solvent in vacuo, and the orange-residue was washed with water, dried under vacuum, and then purified by silica gel column chromatography eluting with a 1:3 mixture of hexane and $CH_2Cl_2$; yield: 112 mg, 0.22 mmol, 60%. Selected spectral data of **LJ5**: $^1$H NMR (500 MHz, $CDCl_3$, 298 K): $\delta$ 7.65 (1H, d, $J_{HH}$=4.0 Hz), 7.43 (2H, d, $J_{HH}$=9.0 Hz), 7.30 (1H, d, $J_{HH}$=4.0 Hz), 7.26 (4H, t, $J_{HH}$=7.8 Hz), 7.18 (1H, d, $J_{HH}$=4.0 Hz), 7.15 (1H, d, $J_{HH}$=3.6 Hz), 7.11–7.03 (8H, m), 3.93 (2H, s). MS (FAB): *m*/*z* 476 ($M^+$). $^{13}$C NMR (125 MHz, $CDCl_3$, 298 K): $\delta$ 178.6, 148.7, 148.1, 147.1, 146.7, 137.8, 134.7, 133.4, 129.4, 127.6, 126.8, 126.6, 124.8, 123.8, 123.5, 123.2, 123.0, 113.5, 29.0. Anal. Calcd for $C_{29}H_{20}N_2OS_2$: C, 73.08; H, 4.23; N, 5.88. Found: C, 72.91; H, 4.59; N, 5.68. IR (neat): 2254, 1653, 1591 cm$^{-1}$.

*4.1.6. 2-Cyano-3-(5-(5′-(4-(diphenylamino)phenyl)-2,2′-bithiophen-5-yl) isoxazol-3-yl) acetic acid (**LJ6**).* Compound **4** (82 mg, 0.16 mmol) was mixed with cyanoacetic acid (CAA, 21 mg, 0.24 mmol), ammonium acetate (19 mg, 0.06 mmol) in glacial acetic acid (10 mL) and the solution was refluxed for 3 h. After cooling to rt, the mixture was poured into water to yield an orange precipitate. This precipitate was collected and washed with water (2×5 mL) and a mixture of 1:1 mixture of hexane and diethylether (5 mL) in sequence. Further purification was conducted by crystallization from a mixture of THF and hexane; yield: 54 mg, 0.10 mmol, 60%. Selected spectral data of **LJ6**: $^1$H NMR (500 MHz, DMSO-$d_6$, 298 K): $\delta$ 8.04 (1H, s), 7.81 (1H, d, $J_{HH}$=4.0 Hz), 7.59 (2H, d, $J_{HH}$=9.0 Hz), 7.49 (1H, d, $J_{HH}$=4.0 Hz), 7.46 (1H, d, $J_{HH}$=4.0 Hz), 7.43 (1H, d, $J_{HH}$=4.0 Hz), 7.34–7.31 (5H, m), 7.10–7.04 (6H, m), 6.97 (2H, d, $J_{HH}$=9.0 Hz). MS (FAB): *m*/*z* 571 ($M^+$). Anal. Calcd for $C_{33}H_{21}N_3O_3S_2\cdot H_2O$: C, 67.21; H, 3.93; N, 7.13. Found: C, 67.09; H, 4.16; N, 7.27.

*4.1.7. 2-(5-(5-(5′-(4-Diphenylaminophenyl)-2,2′-bithiophen-5-yl) isoxazol-3-yl)methylene-4-oxo- 2-thioxothiazolidin-3-yl) acetic acid (**LJ7**).* Compound **4** (82 mg, 0.16 mmol) was mixed with rhodanine-3-acetic acid (RAA, 46 mg, 0.24 mmol) and ammonium acetate (19 mg, 0.06 mmol) in glacial acetic acid (10 mL). The solution was

then refluxed for 3 h. After cooling to rt, the mixture was poured into water to yield a red precipitate. This precipitate was collected and washed with water (3×5 mL) and a mixture of 1:1 mixture of hexane and diethylether (5 mL) in sequence. Further purification was conducted by crystallization from a mixture of THF and hexane; yield: 68 mg, 0.10 mmol, 63%. Selected Spectral data of **LJ7**: $^1$H NMR (500 MHz, DMSO-$d_6$, 298 K): $\delta$ 7.75 (1H, s), 7.74 (1H, d, $J_{HH}$=4.0 Hz), 7.58 (2H, d, $J_{HH}$=8.0 Hz), 7.47 (1H, d, $J_{HH}$=4.0 Hz), 7.44 (1H, d, $J_{HH}$=3.5 Hz), 7.41 (1H, d, $J_{HH}$=3.5 Hz), 7.32 (4H, t, $J_{HH}$=8.0 Hz), 7.21 (1H, s), 7.10–7.04 (6H, m), 6.96 (2H, d, $J_{HH}$=8.5 Hz), 4.69 (2H, s). MS (FAB): $m/z$ 679 ($M^+$). $^{13}$C NMR (125 MHz, $CDCl_3$, 298 K): $\delta$ 172.0, 167.1, 165.7, 165.1, 158.2, 147.2, 146.7, 143.7, 140.1, 133.2, 129.9, 129.6, 129.1, 126.9, 126.6, 126.4, 125.1, 124.9, 124.4, 124.0, 123.6, 122.6, 118.1, 101.4, 45.1. Anal. Calcd for $C_{35}H_{23}N_3O_4S_4\cdot H_2O$: C, 60.41; H, 3.62; N, 6.04. Found: C, 60.76; H, 3.71; N, 6.09.

### 4.2. Fabrication of DSSC and photovoltaic measurements

$TiO_2$ anatase nanoparticles of 20 nm were prepared according to published procedures[28] with slight modification. $TiO_2$ particles were dispersed in α-terpineol with ethyl cellulose as a binder. The $TiO_2$ thin films of 12 μm were prepared by a doctor-blade method on a transparent conducting oxide (F-doped $SnO_2$, FTO). These films were dried at 120 °C for 5 min and then a 4 μm thick layer of 400 nm $TiO_2$ particles (Ti–Nanoxide R/SP paste from Solaronix) was deposited again by a doctor-blade method with a dimension of 0.5×0.5 cm$^2$. Afterward, the double-layered films were sintered at 500 °C for 30 min. After sintering, the $TiO_2$ films were treated with 40 mM of $TiCl_4$ solution, rinsed with water and ethanol, and sintered at 500 °C for 30 min. After cooling to 80 °C, the $TiO_2$ electrode was coated with dyes by dipping into a solution of $3\times10^{-4}$ M of the targeted dye, together with 1 mM of deoxycholic acid (DCA) in DMF solution overnight. After being rinsed with EtOH, the dye-coated $TiO_2$ electrode was assembled into a sandwich-type cell with a Pt-coated FTO as counter electrode and a film (Surlyn 1702, 25 μm) as a spacer between the electrodes. The electrolyte solution was then injected into the cell through a drilled hole in the back of the counter electrode. The hole was then sealed using a hot-melt ionomer film and a cover glass.

The Pt counter electrode was prepared by spin-coating a 0.05 M $H_2PtCl_6$ in isopropyl alcohol solution on FTO glass, followed by sintering at 385 °C for 15–30 min. The liquid electrolyte contained 0.6 M 1-butyl-3-methylimidazolium iodide (BMII), 0.1 M LiI, 0.05 M $I_2$, 0.5 M 4-*tert*-butylpyridine (TBP), 0.1 M guanidinium thiocyanate in dry acetonitrile. Performances of DSSCs were measured with a 0.25 cm$^2$ working area.[29] Light-to-electricity conversion efficiency values were measured using a modified light source, 450 W Xe lamp (Oriel, 6266), an Oriel 81088 Air Mass 1.5 Global filter and a digital source meter purchased from Keithley Instruments Inc. The incident light intensity was calibrated by using a standard solar cell composed of a crystalline silicon solar cell and an IR cutoff filter (Schott, KG-5), giving the photoresponse range of amorphous silicon solar cell. The applied potential and cell current were measured using a Keithley model 2400 digital source meter.

## Supplementary data

Supplementary data associated with this article can be found in online version at doi:10.1016/j.tet.2010.03.085.

## References and notes


1. (a) Robertson, N. *Angew. Chem., Int. Ed.* **2006**, *45*, 2338–2345; (b) Goncalves, L. M.; de Zea Bermudez, V.; Ribeiro, H. A.; Mendes, A. M. *Energy Environ. Sci.* **2008**, *1*, 655–667; (c) Grätzel, M. *Acc. Chem. Res.* **2009**, *42*, 1788–1798.
2. (a) Nazeeruddin, M. K.; Pechy, P.; Renouard, T.; Zakeeruddin, S. M.; Humphry-Baker, R.; Comte, P.; Liska, P.; Cevey, L.; Costa, E.; Shklover, V.; Spiccia, L.; Deacon, G. B.; Bignozzi, C. A.; Graetzel, M. *J. Am. Chem. Soc.* **2001**, *123*, 1613–1624; (b) Nazeeruddin, M. K.; Angelis, F. D.; Fantacci, S.; Selloni, A.; Viscardi, G.; Liska, P.; Ito, S.; Takeru, B.; Grätzel, M. *J. Am. Chem. Soc.* **2005**, *127*, 16835–16847; (c) Chen, C.-Y.; Wang, M.; Li, J.-Y.; Pootrakulchote, N.; Alibabaei, L.; Ngoc-Le, C.-H.; Decoppet, J.-D.; Tsai, J.-H.; Gratzel, C.; Wu, C.-G.; Zakeeruddin, S. M.; Gratzel, M. *ACS Nano* **2009**, *3*, 3103–3109; (d) Chen, B.-S.; Chen, K.; Hong, Y.-H.; Liu, W.-H.; Li, T.-H.; Lai, C.-H.; Chou, P.-T.; Chi, Y.; Lee, G.-H. *Chem. Commun.* **2009**, 5844–5846.
3. (a) Mishra, A.; Fischer, M. K. R.; Bauerle, P. *Angew. Chem., Int. Ed.* **2009**, *48*, 2474–2499; (b) Ooyama, Y.; Harima, Y. *Eur. J. Org. Chem.* **2009**, 2903–2934.
4. (a) Hara, K.; Sato, T.; Katoh, R.; Furube, A.; Ohga, Y.; Shinpo, A.; Suga, S.; Sayama, K.; Sugihara, H.; Arakawa, H. *J. Phys. Chem. B* **2003**, *107*, 597–606; (b) Hara, K.; Wang, Z.-S.; Sato, T.; Furube, A.; Katoh, R.; Sugihara, H.; Dan-oh, Y.; Kasada, C.; Shinpo, A.; Suga, S. *J. Phys. Chem. B* **2005**, *109*, 15476–15482; (c) Wang, Z.-S.; Cui, Y.; Hara, K.; Dan-oh, Y.; Kasada, C.; Shinpo, A. *Adv. Mater.* **2007**, *19*, 1138–1141; (d) Wang, Z.-S.; Cui, Y.; Dan-oh, Y.; Kasada, C.; Shinpo, A.; Hara, K. *J. Phys. Chem. C* **2008**, *112*, 17011–17017.
5. (a) Horiuchi, T.; Miura, H.; Uchida, S. *Chem. Commun.* **2003**, 3036–3037; (b) Horiuchi, T.; Miura, H.; Sumioka, K.; Uchida, S. *J. Am. Chem. Soc.* **2004**, *126*, 12218–12219; (c) Schmidt-Mende, L.; Bach, U.; Humphry-Baker, R.; Horiuchi, T.; Miura, H.; Ito, S.; Uchida, S.; Grätzel, M. *Adv. Mater.* **2005**, *17*, 813–815; (d) Ito, S.; Zakeeruddin, S. M.; Humphry-Baker, R.; Liska, P.; Charvet, R.; Comte, P.; Nazeeruddin, M. K.; Pechy, P.; Takada, M.; Miura, H.; Uchida, S.; Grätzel, M. *Adv. Mater* **2006**, *18*, 1202–1205; (e) Ito, S.; Miura, H.; Uchida, S.; Takata, M.; Sumioka, K.; Liska, P.; Comte, P.; Pechy, P.; Grätzel, M. *Chem. Commun.* **2008**, 5194–5196.
6. (a) Hara, K.; Kurashige, M.; Ito, S.; Shinpo, A.; Suga, S.; Sayama, K.; Arakawa, H. *Chem. Commun.* **2003**, 252–253; (b) Kitamura, T.; Ikeda, M.; Shigaki, K.; Inoue, T.; Anderson, N. A.; Ai, X.; Lian, T.; Yanagida, S. *Chem. Mater.* **2004**, *16*, 1806–1812; (c) Hara, K.; Sato, T.; Katoh, R.; Furube, A.; Yoshihara, T.; Murai, M.; Kurashige, M.; Ito, S.; Shinpo, A.; Suga, S.; Arakawa, H. *Adv. Funct. Mater.* **2005**, *15*, 246–252.
7. (a) Sayama, K.; Tsukagoshi, S.; Hara, K.; Ohga, Y.; Shinpou, A.; Abe, Y.; Suga, S.; Arakawa, H. *J. Phys. Chem. B* **2002**, *106*, 1363–1371; (b) Sayama, K.; Hara, K.; Mori, N.; Satsuki, M.; Suga, S.; Tsukagoshi, S.; Abe, Y.; Sugihara, H.; Arakawa, H. *Chem. Commun.* **2000**, 1173–1174.
8. (a) Yao, Q.-H.; Shan, L.; Li, F.-Y.; Yin, D.-D.; Huang, C.-H. *New J. Chem.* **2003**, *27*, 1277–1283; (b) Chen, Y.-S.; Li, C.; Zeng, Z.-H.; Wang, W.-B.; Wang, X.-S.; Zhang, B.-W. *J. Mater. Chem.* **2005**, *15*, 1654–1661.
9. (a) Xiao, S.; Li, Y.; Li, Y.; Zhuang, J.; Wang, N.; Liu, H.; Ning, B.; Liu, Y.; Lu, F.; Fan, L.; Yang, C.; Li, Y.; Zhu, D. *J. Phys. Chem. B* **2004**, *108*, 16677–16685; (b) Li, Y.; Liu, Y.; Wang, N.; Li, Y.; Liu, H.; Lu, F.; Zhuang, J.; Zhu, D. *Carbon* **2005**, *43*, 1968–1975; (c) Li, C.; Yum, J.-H.; Moon, S.-J.; Herrmann, A.; Eickemeyer, F.; Pschirer, N. G.; Erk, P.; Schoeneboom, J.; Muellen, K.; Grätzel, M.; Nazeeruddin, M. K. *ChemSusChem* **2008**, *1*, 615–618; (d) Imahori, H.; Umeyama, T.; Ito, S. *Acc. Chem. Res.* **2009**, *42*, 1809–1818.
10. Nazeeruddin, M. K.; Humphry-Baker, R.; Officer, D. L.; Campbell, W. M.; Burrell, A. K.; Grätzel, M. *Langmuir* **2004**, *20*, 6514–6517.
11. (a) Kim, S.; Lee, J. K.; Kang, S. O.; Ko, J.; Yum, J.-H.; Fantacci, S.; De Angelis, F.; Censo, D. D.; Nazeeruddin, M. K.; Grätzel, M. *J. Am. Chem. Soc.* **2006**, *128*, 16701–16707; (b) Jung, I.; Lee, J. K.; Song, K. H.; Song, K.; Kang, S. O.; Ko, J. *J. Org. Chem.* **2007**, *72*, 3652–3658; (c) Xu, M.; Li, R.; Pootrakulchote, N.; Shi, D.; Guo, J.; Yi, Z.; Zakeeruddin, S. M.; Grätzel, M.; Wang, P. *J. Phys. Chem. C* **2008**, *112*, 19770–19776.
12. (a) Barbara, P. F.; Mayer, T. J.; Ratner, M. A. *J. Phys. Chem.* **1996**, *100*, 13148–13168; (b) Tian, H.; Yang, X.; Chen, R.; Zhang, R.; Hagfeldt, A.; Sun, L. *J. Phys. Chem. C* **2008**, *112*, 11023–11033.
13. (a) Tian, H.; Yang, X.; Pan, J.; Chen, R.; Liu, M.; Zhang, Q.; Hagfeldt, A.; Sun, L. *Adv. Funct. Mater.* **2008**, *18*, 3461–3468; (b) Baheti, A.; Tyagi, P.; Thomas, K. R. J.; Hsu, Y.-C.; Lin, J. T. *J. Phys. Chem. C* **2009**, *113*, 8541–8547; (c) Marinado, T.; Nonomura, K.; Nissfolk, J.; Karlsson, M. K.; Hagberg, D. P.; Sun, L.; Mori, S.; Hagfeldt, A. *Langmuir* **2010**. doi:10.1021/la902897z
14. (a) Hagberg, D. P.; Edrinsson, T.; Marinado, T.; Boschloo, G.; Hagfeldt, A.; Sun, L. *Chem. Commun.* **2006**, 2245–2247; (b) Kim, S.; Choi, H.; Baik, C.; Song, K.; Kang, S. O.; Ko, J. *Tetrahedron* **2007**, *63*, 11436–11443; (c) Liu, W.-H.; Wu, I.-C.; Lai, C.-H.; Lai, C.-H.; Chou, P.-T.; Li, Y.-T.; Chen, C.-L.; Hsu, Y.-Y.; Chi, Y. *Chem. Commun.* **2008**, 5152–5154; (d) Qin, H.; Wenger, S.; Xu, M.; Gao, F.; Jing, X.; Wang, P.; Zakeeruddin, S. M.; Gratzel, M. *J. Am. Chem. Soc.* **2008**, *130*, 9202–9203; (e) Wang, M.; Xu, M.; Shi, D.; Li, R.; Gao, F.; Zhang, G.; Yi, Z.; Humphry-Baker, R.; Wang, P.; Zakeeruddin, S. M.; Grätzel, M. *Adv. Mater.* **2008**, *20*, 4460–4463; (f) Xi, C.; Cao, Y.; Cheng, Y.; Wang, M.; Jing, X.; Zakeeruddin, S. M.; Grätzel, M.; Wang, P. *J. Phys. Chem. C* **2008**, *112*, 11063–11067; (g) Thomas, K. R. J.; Hsu, Y.-C.; Lin, J. T.; Lee, K.-M.; Ho, K.-C.; Lai, C.-H.; Cheng, Y.-M.; Chou, P.-T. *Chem. Mater.* **2008**, *20*, 1830–1840; (h) Xu, M.; Wenger, S.; Bala, H.; Shi, D.; Li, R.; Zhou, Y.; Zakeeruddin, S. M.; Gratzel, M.; Wang, P. *J. Phys. Chem. C* **2009**, *113*, 2966–2973; (i) Zhang, G.; Bai, Y.; Li, R.; Shi, D.; Wenger, S.; Zakeeruddin, S. M.; Grätzel, M.; Wang, P. *Energy Environ. Sci.* **2009**, *2*, 92–95; (j) Yang, H.-Y.; Yen, Y.-S.; Hsu, Y.-C.; Chou, H.-H.; Lin, J. T. *Org. Lett.* **2010**, *12*, 16–19.
15. Zang, G.; Bala, H.; Cheng, Y.; Shi, D.; Lv, X.; Yu, Q.; Wang, P. *Chem. Commun.* **2009**, 2198–2200.
16. (a) Kuang, D.; Uchida, S.; Hamphry-Baker, R.; Zakeeruddin, S. M.; Grätzel, M. *Angew. Chem., Int. Ed.* **2008**, *47*, 1923–1927; (b) Marinado, T.; Hagberg, D. P.; Hedlund, M.; Edvinsson, T.; Johansson, E. M. J.; Boschloo, G.; Rensmo, H.; Brinck, T.; Sun, L.; Hagfeldt, A. *Phys. Chem. Chem. Phys.* **2009**, *11*, 133–141.

17. (a) Bettenhausen, J.; Strohriegl, P.; Brütting, W.; Tokuhisa, H.; Tsutsui, T. *J. Appl. Phys.* **1997**, *82*, 4957–4961; (b) Yasuda, T.; Yamaguchi, Y.; Zou, D.-C.; Tsutsui, T. *Jpn. J. Appl. Phys., Part 1* **2002**, *41*, 5626–5629.
18. (a) Ning, Z.; Tian, H. *Chem. Commun.* **2009**, 5483–5495; (b) Preat, J.; Michaux, C.; Jaxquemin, D.; Perpète, E. A. *J. Phys. Chem. C* **2009**, *113*, 16821–16833.
19. (a) Kozikowski, A. P.; Adamcz, M. *J. Org. Chem.* **1983**, *48*, 366–372; (b) Reuman, M.; Beish, S.; Davis, J.; Batchelor, M. J.; Hutchings, M. C.; Moffat, D. F. C.; Connolly, P. J.; Russell, R. K. *J. Org. Chem.* **2008**, *73*, 1121–1123.
20. Tian, H.; Yang, X.; Chen, R.; Pan, Y.; Li, L.; Hagfeldt, A.; Sun, L. *Chem. Commun.* **2007**, 3741–3743.
21. (a) Velusamy, M.; Thomas, K. R. J.; Lin, J. T.; Hsu, Y.-C.; Ho, K.-C. *Org. Lett.* **2005**, *7*, 1899–1902; (b) Kim, D.; Kang, M.-S.; Song, K.; Kang, S. O.; Ko, J. *Tetrahedron* **2008**, *64*, 10417–10424; (c) Hara, K.; Sayama, K.; Ohga, Y.; Shinpo, A.; Suga, S.; Arakawa, H. *Chem. Commun.* **2001**, 569–570; (d) Chen, K.-S.; Liu, W.-H.; Wang, Y.-H.; Lai, C.-H.; Chou, P.-T.; Chen, K.; Chi, Y. *Adv. Funct. Mater.* **2007**, *17*, 2964–2974.
22. Hagfeldt, A.; Grätzel, M. *Chem. Rev.* **1995**, *95*, 49–68.
23. Boschloo, G.; Haeggman, L.; Hagfeldt, A. *J. Phys. Chem. B* **2006**, *110*, 13144–13150.
24. (a) Liang, M.; Xu, W.; Cai, F.; Chen, P.; Peng, B.; Chen, J.; Li, X. *J. Phys. Chem. C* **2007**, *111*, 4465–4472; (b) Wiberg, J.; Marinado, T.; Hagberg, D. P.; Sun, L.; Hagfeldt, A.; Albinsson, B. *J. Phys. Chem. C* **2009**, *113*, 3881–3886.
25. Chung, W.-T.; Chen, B.-S.; Chen, K.-Y.; Hsieh, C.-C.; Chou, P.-T. *Chem. Commun.* **2009**, 6982–6984.
26. Wang, Q.; Moser, J.-E.; Grätzel, M. *J. Phys. Chem. B* **2005**, *109*, 14945–14953.
27. (a) Cherioux, F.; Guyard, L. *Adv. Funct. Mater* **2001**, *11*, 305–309; (b) Nenajdenko, V. G.; Baraznenok, I. L.; Balenkova, E. S. *J. Org. Chem.* **1998**, *63*, 6132–6136.
28. Wang, P.; Zakeeruddin, S. M.; Comte, P.; Charvet, R.; Humphry-Baker, R.; Grätzel, M. *J. Phys. Chem. B* **2003**, *107*, 14336–14341.
29. Ito, S.; Nazeeruddin, M. K.; Liska, P.; Comte, P.; Charvet, R.; Péchy, P.; Jirousek, M.; Kay, A.; Zakeeruddin, S. M.; Grätzel, M. *Prog. Photovoltaics Res. Appl.* **2006**, *14*, 589–601.